International Journal of Science and Research (IJSR)
ISSN (Online): 2319-7064
Index Copernicus Value (2013): 6.14 | Impact Factor (2014): 5.611

Bearing Capacity of Sand Overlying Clay – Strip Footing

Mohamed I. Ramadan[1], Mohammed H. Hussien[2]

[1]Civil Engineering Department, Faculty of Engineering-Rabigh, King Abdulaziz University, KSA
Civil Engineering Department, Faculty of Engineering, Assiut University, Assiut, Egypt

[2]Civil Engineering Department, Faculty of Engineering, Assiut University, Assiut, Egypt

Abstract: ***Soil naturally occurs in deposited layers. Each layer of the soil may be assumed to be homogeneous, although the strength properties of adjacent layers are quite different. The present study aims mainly to investigate the behavior of footing under vertical central load placed on the surface of two layered soil. The study has been carried out for the bearing capacity of sand overlying clay. Experimental and numerical works have been carried out. A review of previous researches is given and a discussion is presented of the dimensionless relationships that govern the behavior of this type of foundation. The results are presented in terms of the ultimate bearing capacity, load-settlement curves, and non-dimensional relationships to show the effect of upper layer thickness to footing width ratio, (H/B), and the strength of the upper layer soil on the bearing capacity. In addition, modes of failure of the foundation soil system are also presented.***

Keywords: bearing capacity, sand overlying clay, sand thickness ratio; mode of failure**.**

1. Introduction

Several important examples exist for foundation engineering problems where it may be necessary to include the effect of soil layers in the assessment of bearing capacity. Shallow offshore foundations and raft foundations, for example, generally have large physical dimensions; potential failure surfaces may therefore extend to a significant distance below the soil surface. It is expected that any soil layer within the depth of these failure surfaces would be influenced by the failure load. Other examples include structures placed on engineered fill layers as oil storage tanks, which may be founded on a thin layer of granular fill and unpaved roads built on soft clay where a layer of compacted fill is used to spread the load applied by the passing vehicles.

A very common kind of soil non-homogeneity is that of distinct soil layers of different strength and approximately constant thickness. The simplest situations that can be considered would be those of a two-layer profile in two characteristic conditions:
a) Bearing stratum is softer than the underlying stratum, Fig. (1.a);
b) Bearing stratum is stiffer than the underlying stratum, Fig. (1.b).

Extensive research work has been done for the behavior of the sand overlying clay. Most of the available design methods are analytical approaches based on experimental work.

In the present study, laboratory plane strain bearing tests were performed and finite element simulations of these tests using the finite element program PLAXIS 3D Tunnel were carried out to investigate the actual behavior and mode of failure of sand overlying clay under a vertical central load. Comparisons between numerical and experimental results are presented to assure that the development of such FEM model will help in the investigation of prototype cases.

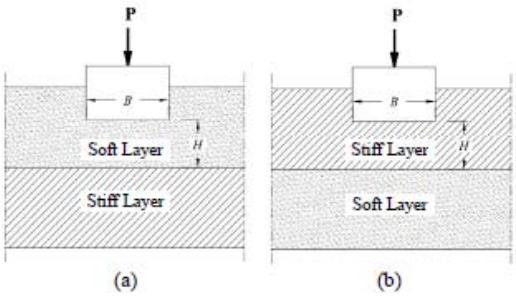

Figure 1: Typical two-layer soils profiles

2. Previous Research

2.1 Experimental Research

Laboratory model tests were carried out by many investigators, e.g. Dembicki and Odrobinski [1], Hanna [2], Abdrabbo et al. [3], and Kenny and Andrawes [4], and Ramadan [5]. Centrifuge tests were performed by others as Okamura et al. [6], and Brown et al. [7]. The main conclusions of these studies can be summarized as follows:

1) Changing the composition of soil from a dense sand bed to dense sand layer overlying medium clay cause the mode of failure for the surface footing to change from general shear failure to punching shear failure in the upper sand associated with local shear failure in the underlying clay. However, footing resting on soil composed of medium to compacted sand overlying medium to soft clay; local shear failure takes place.
2) The thickness ratio $(H/B)_{crit.}$ of the upper sand layer, at which the clay layer does not participate in the bearing capacity of the surface footing placed on a sand overlying clay, is dependent on the shear strength of the clay, relative density of sand, and on the footing-soil system strain level.
3) For the cases of punching shear, the side angle to the vertical of the sand block, α, increases by increasing H/B

and overburden pressure, and by decreasing strength of clay. These results are inconsistent with the assumption of constant α which is adopted in most existing methods of bearing capacity calculations.

4) Observed vertical stresses on the clay surface beneath the sand block at the peak load are higher than the bearing capacity of footing on the clay.

2.2 Analytical approaches

Analytical approaches were proposed for computing the bearing capacity of sand overlying clay. A method called the projected area method was proposed by Yamaguchi; as reported by [8]; as shown in Fig. (2.a). In this method, the shearing resistance of sand along the side of the sand block was neglected. The side angles of the block as proposed by various researchers [9] are different from each other; for example, 30° for Yamaguchi, $\tan^{-1}$ 0.5 for Terzaghi and Peck, and Kraft and Helfrich, 30° and 45° for Myslivec and Kysela and ϕ for Baglioni. These angles are assumed constant irrespective of the strengths of the soils and geometric conditions, except for that proposed by Baglioni [9].

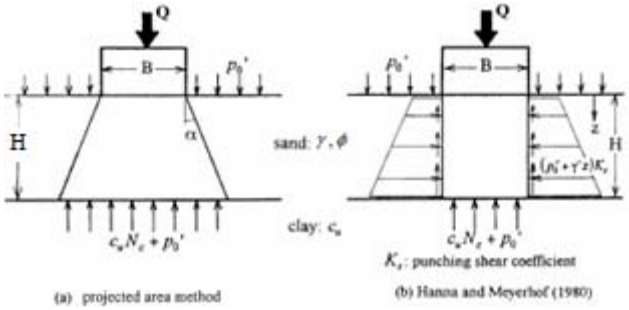

Figure 2: Mechanisms adopted in existing methods of analysis, (After *Okamura et al.*, [13])

A punching shear model proposed by Meyerhof [10] and Hanna and Meyerhof [11] was based on well-established theory and provides a useful insight into the behavior of granular soils overlying clay, as shown in Fig. (2.b). They suggested the following equation to calculate the ultimate bearing capacity of a strip footing in case of punching shear failure:

$$q_u = cN_c + \gamma H^2\left(1+\frac{2D_f}{H}\right)K_s\frac{\tan\phi}{B} + \gamma D_f \qquad (1)$$

where; D_f = overburden soil depth.

Das [10] set that K_s depends on the angle of internal friction of the sand layer. While Burd and Frydman [11], and Kenny and Andrawes [4] set that according to Hanna and Meyerhof [11] K_s depends on the mobilized angle of friction δ, the undrained shear strength of the clay c_u, the angle of friction of the sand, ϕ, and the bearing capacity ratio q_s / q_c. This model may be compared to a simple load spread approach if it is assumed that the load from the footing is spread over a total width B' at the base of the sand and that the bearing stress at the clay surface is $N_c\, c_u + \gamma D_f$. The punching shear model then gives:

$$B' = B + \frac{\gamma D^2 K_s \tan\phi}{N_c c_u} \qquad (2)$$

$$\tan\beta = \left(\frac{\gamma D}{c_u}\right)\left(\frac{K_s \tan\phi}{2N_c}\right) \qquad (3)$$

Okamura et al. [8] compared the factors as thickness of sand, strength of clay and width, shape and embedment of footing, as well as calculated bearing capacities to the results of well-conditioned centrifuge tests by [6] to verify the validity of the previous methods. It has been confirmed that reasonable assumptions in which the variation of the shape of the sand block and the forces related to the factors taken into consideration are important to obtain a reasonable prediction, as shown in Fig.(3).

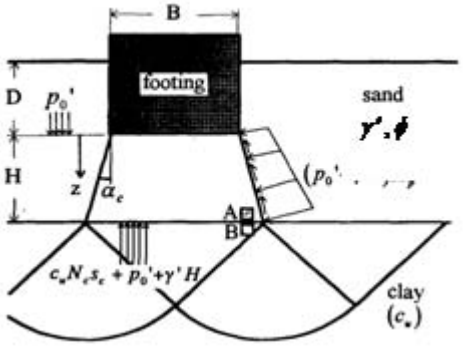

Figure 3: Failure mechanism assumed in proposed method, (After *Okamura et al.*, [13])

In their study, a new limit equilibrium method has been proposed in order to overcome the problems, which exist in the assumptions made in the previous methods, Fig. (3). To incorporate the influence of stress level on friction angle, they proposed calculating the friction angle ϕ through an iterative procedure between ϕ and the initial mean effective stress at the mid-depth of the sand layer, with the assumption that the normal stress at the slip surface is at a passive failure state.

3. Experimental Work

Dry sand and wet clay were used as upper and lower soil layers, respectively. Sand was a silica sand of maximum and minimum dry unit weights of 18.0 and 15.6 kN/m^3, respectively. It has a specific gravity of 2.65. Two relative densities were achieved in the tests; dense sand of 90% relative density and loose sand of 30% relative density. The triaxial angles of internal friction of dense and loose sand were 42° and 35.25°, respectively. For clay layer, it's mainly contents are 56.7% of clay, 35.3% of silt and 8% of sand. It has a specific gravity of 2.71, dry unit weight of 13.4 kN/m^3,

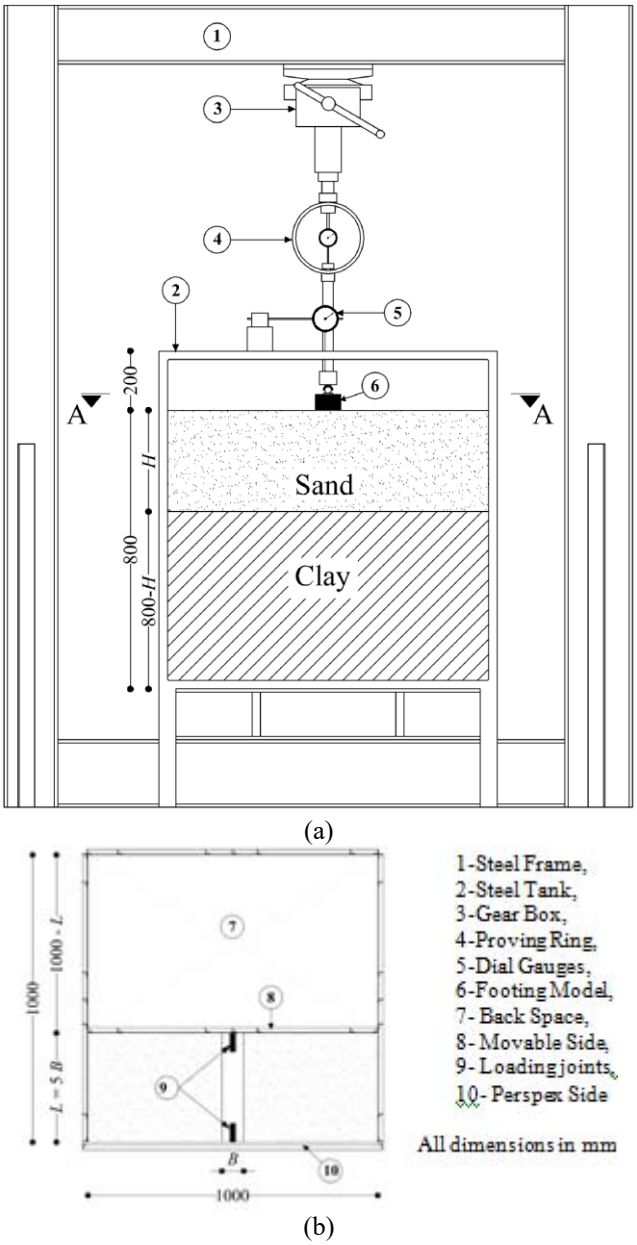

Figure 4: Test Setup: (a) Elevation, (b) Section A-A

liquid limit of 55%, and plastic limit of 27%. It was prepared at water content of 34.3%. Undrained shear strength from unconfined compression test, c_u is 32 kN/m^2.

The assembly drawing of the experimental apparatus is shown in Fig. (4). The figure shows a rigid steel frame (1) and a steel tank (2), 1 x 1 x 1 m used as a soil container with a movable back side can be fixed to adjust the end of the footing to give the plane strain condition. Eleven tests were carried out to investigate the bearing capacity of sand overlying clay under isolated surface strip footing with two different widths. The testing program is shown in Table (1).

Soil was placed in the tank in layers in a manner to achieve the placement properties. The loads were applied incrementally with a controlled displacement rate and the displacements of the footing were recorded. Digital photos were taken before and after loading to observe the behavior of sand overlying clay, mode of the failure, and dimensions of the rupture zone. The loading was stopped after sudden big drop in the proving ring reading or after settlement = 40% of the footing width, (S/B = 40%), as set by Okamura [6], except for case of using loose sand as upper layer, where

Table 1: Testing program

Test No.	Footing width, B (mm)	Soil layers system	H/B
1	75	Dense Sand overlying Clay	0
2			1
3			3
4	75	Loose Sand overlying Clay	1
5			3
6	100	Dense Sand overlying Clay	0
7			1
8			3
9			∞
10	100	Loose Sand overlying Clay	1
11			3

S/B did not exceed 20%. For more details about experimental test setup and soil preparation, it can be referred to Ramadan [5].

4. Finite Element Simulation

Both experimental and numerical studies complete each other in dealing with scientific researches. Finite element modeling has more advantages than experimental modeling those parameters may be varied easily and details of stresses and deformations throughout the system may be studied. This is particularly valuable for investigating the mechanisms and the effective stresses developing in the two-layer soils system, which is extremely difficult to do in a model test.

A three-dimensional finite element simulation for the experimental tests, using PLAXIS 3D Tunnel program [12], was carried out to investigate the actual behavior of the two-layer soils system, sand overlying medium clay, under plane strain conditions. Figure (5) shows the problem notations to know the factors affecting the problem.

4.1 Geometry and Meshing

All tests of the same footing width, B were conducted using the same mesh, number of elements, number of nodes, number of degree of freedom, and number of stress points. The model geometry and meshing for footing width, B = 100 mm is shown in Fig. (6). The model was simulated with the full width of the tank, as the unsymmetrical condition, due to the roller connection between the loading shaft and the footing model in the experimental work, allows the footing rotation. Half-length of the footing was simulated to reduce the number of elements and reduce the time of calculations.

4.2 Modeling and Parameters

Material models and the input parameters of the FEM program are shown in Table (2). All parameters are given

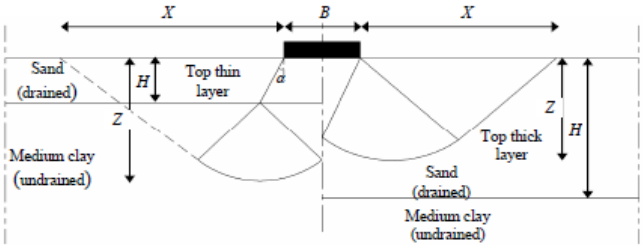

Figure 5: Problem notations and potential failure mechanisms

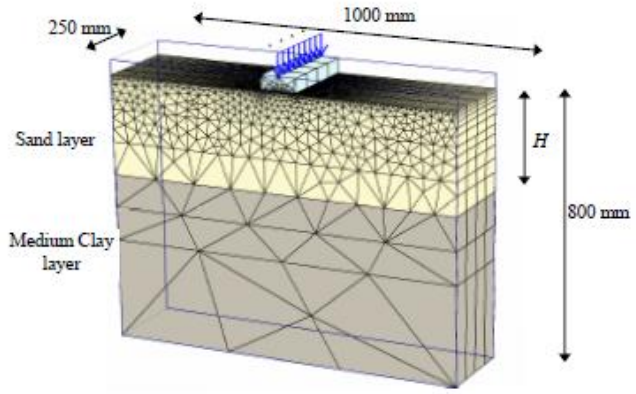

Figure 6: Geometry and meshing for tests of footing width, B = 100 mm

for plane strain condition as suggested by Brocklehurst [13]. The modulus of elasticity, E was calculated from triaxial test stress-strain curves as a secant modulus at 50% strength, E_{50} according to PLAXIS 3D Tunnel [12]. The cohesion parameter of sand was calculated according to Michalowski and Zhu [14]. The value of dilatancy angle of dense sand, (ψ) was obtained from the following equation as recommended by Wan [15]:

$$\psi = \frac{\phi_p - \phi_{cr}}{0.4} \quad (4)$$

where; ϕ_p is The peak angle of internal friction = the calculated angle of internal friction from triaxial test at peak state, and ϕ_{cr} is the angle of internal friction which calculated from triaxial test at critical state.

5. Results of Experimental Tests and FEM Simulation

A wide range of results can be obtained from the finite element simulation. But in this paper the present finite element results will be limited to that can be obtained from the experimental work.

5.1 Dense Sand Overlying Medium Clay

The load-settlement relationships of the footing were obtained from loading tests of both experimental and FEM work. Figure (7) shows these results for B = 100 mm as an example. It was found that in case of a footing resting on medium clay bed or a sand overlying clay with thickness ratio, H/B = 1, it is difficult for local and punching shear failures to establish the failure load. The failure load, for these cases, was determined by plotting the settlement against the load on a log-log scale where the curve consists of an upper curved part and a lower part, which is a straight line. The intersection of these two lines is considered as the rupture point, Hanna [2]. In case of the footing resting on a sand overlying clay with H/B = 3 or dense sand alone; H/B = ∞, there was no difficulty in determining the failure load at the peak point.

Table 2: Input parameters for plane strain condition of the FEM program

Parameter	Dense Sand	Loose Sand	Medium Clay	Footing
Material model	Mohr-Coulomb	Mohr-Coulomb	Mohr-Coulomb	Linear Elastic
Material behavior	Drained	Drained	Undrained	Non-porous
Unit weight, γ, kN/m^3	17.76	16.29	17.90	42.15[a] / 34.53[b]
Young's modulus, E, kN/m^2	20000	2000	4000	2.1E08
Poisson's ratio, v	0.30	0.20	0.35	0.20
Cohesion, c, kN/m^2	0.75[a] / 1.0[b]	0.2	36.0	—
Friction angle, ϕ	47.25	39.66	0	—
Dilatancy angle, ψ	14.625	0	0	—

a: Case of footing width, B = 75 mm
b: Case of footing width, B = 100 mm

5.2 Loose Sand Overlying Medium Clay

The load-settlement relationships of the footing were derived from series of loading tests from both experimental and FEM work. Figure (9) shows the results for B = 100 mm. It was found from all results that the curves are semi linear and it was difficult to inspect the failure point. Therefore, the failure load was selected at S/B = 10 % in the experimental work as suggested by Vesic [9]. In case of FEM, the maximum S/B was generally less than 10 %. The failure load was selected as the maximum load except in case of H/B=3 for B=75 mm the failure load was selected at S/B = 5.15 % as the same ratio reached in other tests.

The values of the ultimate bearing capacity, q_u and the corresponding settlement ratios, S/B %, for both B = 75 mm and B = 100 mm, are shown in Table (3) to clear the comparison between the experimental work and FEM. Both the experimental work and FEM give almost the same behavior.

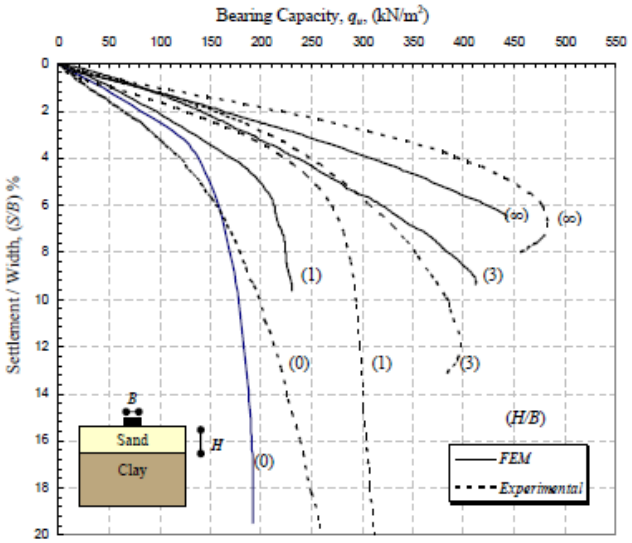

Figure 7: Load-settlement curves from experimental work and FEM for dense sand overlying medium clay, B = 100 mm

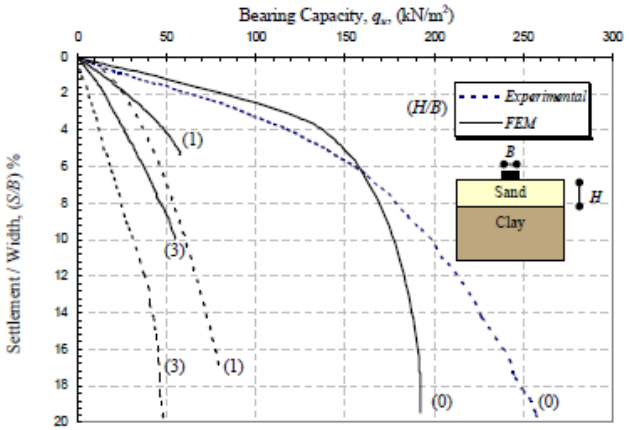

Figure 8: Load-settlement curves from experimental work and FEM for loose sand overlying medium clay, B = 100 mm

Table 3: Values of ultimate bearing capacity, q_u and the corresponding settlement ratio, S/B % for case of (dense/loose) sand overlying medium clay

Sand Thickness Ratio, H/B		*0 (Medium Clay)*		*1*		*3*	
Analysis Type		Exp.	FEM	Exp.	FEM	Exp.	FEM
B= 75 mm	q_u (kN/m^2)	161.4	174.8	188.3/67	205.1/51.5	293.9/42	360.7/30.2
	S/B%	5.66	9.92	14.7/ 10	7.23/ 5.2	11.28/ 10	10.27/5.15
B= 100 mm	q_u (kN/m^2)	162	157	245/ 59.6	218/ 56	398/ 31.4	412.4/32.25
	S/B %	6.53	5.88	4.8/ 10	6.86/ 5.15	11.84/10	9.3/ 5.1

6. Analysis and Discussion of the Results

The following subsections deal with the discussion of the obtained and concluded results from the load-settlement curves, modes of failure and deformations.

6.1 Effect of Sand Layer Thickness Ratio, *H/B*

It was concluded from Fig. (7) and Table (3) that, as the thickness of the upper dense sand layer increases from H/B = 1 to H/B = 3, the ultimate bearing capacity; q_u increases.

The obtained ultimate bearing capacity, q_u has the peak value for the case of H/B = 3 as in the case of H/B = ∞ (sand only). Therefore, in case of dense sand layer overlying medium clay, it is clear that q_u at H/B = 3 is close to the critical thickness ratio, $(H/B)_{crit}$. This means that if H/B increases than $(H/B)_{crit}$, the presence of the clay layer has no effect on the bearing capacity. In other words the bearing capacity at $(H/B)_{crit}$ approximately equals to that at H/B = ∞.

From Fig. (8) and Table (3), as the thickness of loose sand layer increases from H/B = 1 to H/B = 3 the ultimate bearing capacity, q_u decreases. The medium clay layer is considered as a relatively stiff base. It is clear that the critical thickness ratio, $(H/B)_{crit}$ in case of loose sand layer overlying medium clay is between H/B = 1 and H/B = 3. In this case, the increase of height of the loose sand layer is accompanied by large deformations in sand and consequently the bearing capacity decreases.

6.2 Effect of Footing Size, *B*

Figure (9) shows the effect of footing size, B on the ultimate bearing capacity of dense sand overlying medium clay. The relationship is shown as a dimensionless relation between q_u / q'_{clay} and the thickness ratio, H/B, where q'_{clay} = ultimate bearing capacity of the medium clay from model tests. It can be concluded that by increasing the width of the footing the ultimate bearing capacity for dense sand overlying medium clay system increases. The rate of the increase increases by increasing the thickness ratio, H/B.

The effect of footing size, B on q_u of loose sand overlying medium clay is also shown in Fig. (9). It can be concluded that by increasing the width of the footing the ultimate bearing capacity of loose sand overlying medium clay system decreases. The rate of the decrease decreases by increasing the thickness ratio, H/B. This is as the clay, in case of surface footing and undrained condition, has a constant strength; $q_{clay} = c_u N_c$ the width has no effect on the bearing capacity. As the thickness of dense or loose sand layer increases, the participation of the clay layer decreases and the size effect increases, $q_u = c_u N_c + \gamma H + 0.5\gamma B N_\gamma$, where γ = unit weight of the dense sand. However, in the case of loose sand overlying medium clay, if $H/B \geq 1$, where the effect of medium clay layer is decreasing, the rate of decreasing is somewhat constant. As the loose sand layer is weaker than medium clay, the term $(0.5\gamma B N_\gamma)$ has a small effect on q_u comparing with the term $(c_u N_c + \gamma H)$.

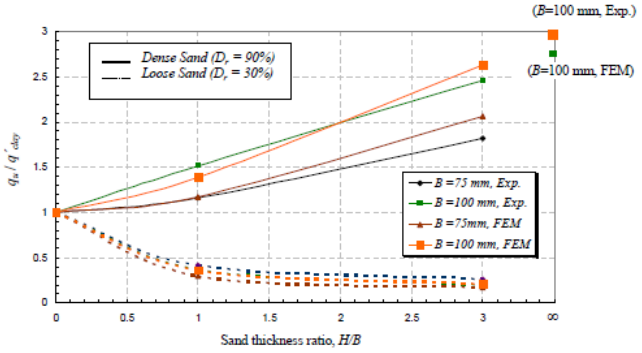

Figure 9: Effect of footing size and relative density of sand, case of sand overlying medium clay

6.3 Effect of Sand Relative Density, D_r

Figure (9) shows the effect of increasing the relative density, D_r on the ultimate bearing capacity of sand overlying medium clay, for both footing widths. It can be concluded that as increasing the relative density of the sand layer q_u increases with high rate especially if H/B increased. Thus, it is important to be careful with improving the bearing capacity of surface footing resting on medium clay soil by placing sand cushion. This sand cushion should be compacted to a high relative density to improve the bearing capacity.

6.4 Modes of Failure and Deformations

Deformed zone observed in the experimental model tests, shear strains and total incremental displacements obtained from FEM give the mode of failure and the dimensions of the rupture zone. Table (4) shows the dimension ratios X/B, Z/B of the rupture zones, values of the side angle of the block in the upper layer, α as indicated in Fig. (5), and type of failure for each case from experimental and FEM.

For dense sand overlying medium clay case, H/B=1, B=100 mm. The medium clay layer is relatively weaker than the dense sand layer. This can be concluded from both the failure patterns observed from experimental work, and shear strains from FEM. A punching shear failure was clearly observed in case of H/B = 1 and B = 100 mm as shown in Figs. (10) and (11).

7. Comparison with Previous Research

The bearing capacity obtained from both experimental work and FEM were compared with that from equations suggested by some authors, as shown in Fig. (12) as a dimensionless relationship between $c_u/\gamma B$ and $q_u/\gamma B$ where γ = unit weight of the sand layer.

It can be observed that both equations suggested by Meyerhof [10] and by Jacobsen [9] give a good agreement with the results of both experimental work and FEM in case of H/B = 1, while in case of H/B = 3 (not shown h) both equations underestimate the bearing capacity especially in the case of the smaller value of cu /γB. Equation suggested by Okamura [13] give a good agreement results with both experimental work and FEM results in case of H/B = 1 and 3 especially in the case of the small value of cu /γB, while the equation suggested by Terzaghi and Peck [9] highly overestimates the bearing capacity value in all results.

Table 4: Mode of failure and dimensions of rupture zone

Sand Thickness Ratio, H/B			*0 (Medium Clay)*			*1*			*3*		
Analysis Type			Exp.	FEM	Mode of Failure	Exp.	FEM	Mode of Failure	Exp.	FEM	Mode of Failure
Dense Sand overlying Medium Clay	*B* = 75 mm	*X/B*	—	—	*Local shear failure*	—	2.23	*Punching shear failure in sand and local in clay*	4.17	4.9	*General shear failure in sand*
		Z/B	0.7	0.7		2-Jan	1.5		1.45	2	
		α	—	—		14˚	10˚		—	—	
	B = 100 mm	*X/B*	—	—	*Local shear failure*	—	4	*Punching shear failure in sand and local in clay*	3.95	4.5	*General shear failure in sand*
		Z/B	0.7	0.7		1 to 1.5	1.5		1.5	1.65	
		α	—	—		7˚, 10˚	9˚		—	—	
Loose Sand overlying Medium Clay	*B* = 75 mm	*X/B*				1.6	1.85	*General shear failure in sand*	—	—	*Local shear failure in sand*
		Z/B				0.6	0.9		1.6	1.33	
		α				—	—		—	—	
	B = 100 mm	*X/B*				—	1.9	*General shear failure in sand*	—	—	*Local shear failure in sand*
		Z/B				1	1		—	1.50≈	
		α				—	—		—	—	

For case of loose sand overlying medium clay, the comparison of the obtained results showed that all the previous results suggested by authors highly overestimate the bearing capacity values. This can be interpreted as some authors based their equations on the case of punching shear failure, while in case of loose sand overlying medium clay and H/B = 1, general shear failure occurs as the medium clay layer works as a relatively stiff base. In the case of local shear failure, H/B = 3 the clay layer has no effect on the bearing capacity value.

8. Conclusions

Strip surface footings under the effect of vertical central load on sand overlying clay were investigated experimentally and numerically. The following main conclusions can be drawn:

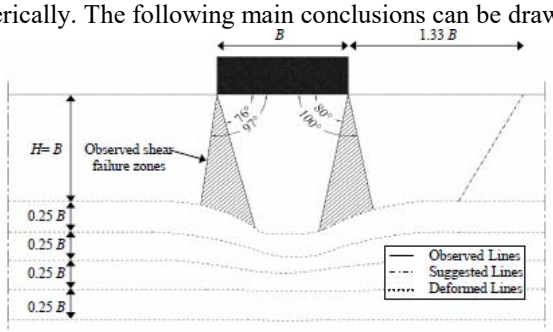

Figure 10: Deformations after loading from experimental work, *H/B*=1, dense sand overlying medium clay, B= 100 mm

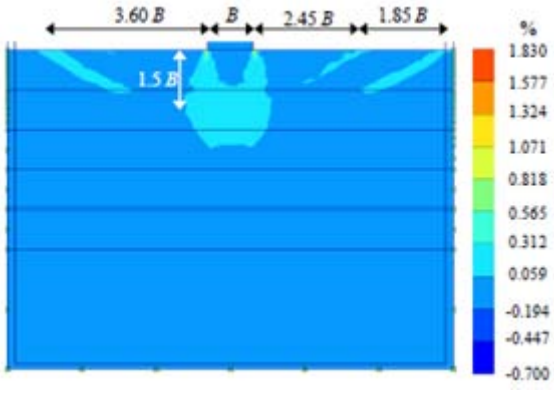

Figure 11: Incremental shear strains, *H/B*=1, dense sand overlying medium clay, B= 100 mm

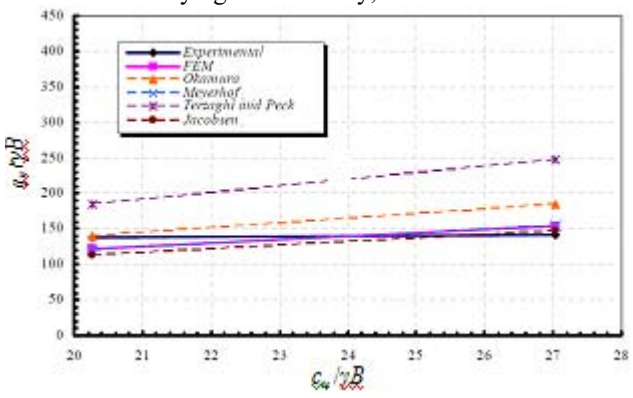

Figure 12: Comparison of bearing capacity of strip footing of dense sand overlying clay with other authors for, *H/B* = 1

1. The ultimate bearing capacity of dense sand overlying medium clay increases as increasing the sand thickness ratio, *H/B*, and width of footing, *B*.
2. The ultimate bearing capacity of loose sand overlying medium clay decreases as increasing the sand thickness ratio, *H/B*. However, width of footing has a small effect on the bearing capacity.
3. The ultimate bearing capacity of sand overlying clay increases by increasing the relative density of upper sand layer.
4. Punching shear failure occurs in upper dense sand layer followed by local shear failure in lower clay layer in case of *H/B* = 1. Whereas general shear failure was observed at *H/B* = 3 and for sand bed only, *H/B* = ∞.
5. General shear failure was observed in upper loose sand layer at *H/B* = 1 which is changed to local shear failure in case of *H/B* = 3.
6. The obtained critical sand thickness ratio, $(H/B)_{crit}$ from model tests cannot be applied for most prototype case. The critical values were observed at high value of $c_u/\gamma B$. This means that by increasing footing width, B, the ratio$(H/B)_{crit}$ will not occur at the same observed values of $c_u/\gamma B$ for the model tests.

9. References

[1] Dembicki, E. and Odrobinski, W. (1973) "A Contribution to the Tests on the Bearing Capacity of Stratified Subsoil under the Foundations", Proc. 8th ICSMFE, Vol. 1, Part 3, 61-64
[2] Hanna, A. (1981) "Experimental Study of Footings in Layered Soil", Journal of Geotechnical Engineering, ASCE, Vol. 107, No. GT8, 1113-1127.
[3] Abdrabo, F. M, Mahmoud, M. A., El-Hansy, R. M., and Kotait, H. A. (1994) "An Experimental Study on Strip Footing Resting on a Stratified Soil", Second Alexandria Conference on Structural and Geotechnical Engineering, 233-246.
[4] Kenny, M. J., and Andrawes, K. Z. (1997) "The Bearing Capacity of a Sand Layer Overlying Soft Clay", Geotechnique 47, No. 2, 339-345.
[5] Ramadan, M. I. H. (2006) "Bearing Capacity and Shape of Failure for Layered Soils under Isolated Footings", M. Sc. Thesis, submitted for examination, Assiut University, Assiut, EGYPT.
[6] Okamura, M., Takemura, J., and Kimura, T. (1997) "Centrifuge Model Tests on Bearing Capacity and Deformation of Sand Layer Overlying Clay", Soils and Foundations, Vol. 37, No. 1, 73-88.
[7] Brown, R., Valsangkar, A. J., and Schriver, A. B., (2004) "Centrifuge Modeling of Surface Footings on Sand Layer Underlain by a Rigid Base", Journal of Geotechnical and Geological Engineering, Vol. 22, 187-198.
[8] Okamura, M., Takemura, J., and Kimura, T. (1998) "Bearing Capacity Predictions of Sand Overlying Clay Based on Limit Equilibrium Method", Soils and Foundations, Vol. 38, No. 1, 181-194.
[9] Winterkorn, H. F., and Fang, H. Y. (1975) "Foundation Engineering Handbook" (EDS), New York, Reinhold.
[10] Das, B. M. (1984) "Principles of Foundation Engineering", Brooks/Cole Engineering Division, Monterey, California.
[11] Burd, H. J., and Frydman, S. (1997) "Bearing Capacity of Plane-Strain Footings on Layered Soils", Canadian Geotechnical Journal, Vol. 34, 241-253.
[12] PLAXIS 3D Tunnel Manual, version 1 (2001) "Finite Element Code for Soil and Rock Analysis", A. A. Balkema Publishers.
[13] Brocklehurst, C. J. (1993) "Finite Element Studies of Reinforced and Unreinforced Two-Layer Soil Systems", Ph. D. Thesis, University of Oxford, Oxford, U. K.

[14] Michalowski, R. L., and Zhu, M. (2005) "Shape Factor for Limit Loads on Square and Rectangular Footings", Journal of Geotechnical Engineering, ASCE, Vol. 131, No. 2, 223-231.
[15] Wan, R. G., Al-Mamun, M., and Guo. P. J. (2005) "How Do Fabric and Dilatancy Affect the Strength of Granular Materials", Proc. 15th ICSMFE, 863-868.

Author Profile

Mohamed I. Ramadan received the B.S. and M.S. degrees in Civil Engineering from Assiut University in 2002 and 2006, respectively. In 2007, he started his PhD studies at Memorial University of Newfoundland, Canada. He performed hid PhD research in offshore geotechnical engineering. In 2011, he obtained his PhD in geotechnical engineering. He is currently working as Assistant Professor at King Abdulaziz University, KSA.

Mohammad H. Hussien received the B.S. and M.S. degrees in Civil Engineering from Assiut University in 1980 and 1987, respectively. He obtained his PhD in in 1996. He is currently working as Associate Professor at Assiut University, Egypt.